Electronic Supporting Information for: Atoms-to-Microns Model for Small Solute Transport through Sticky Nanochannels

Rogan Carr[α‡], Jeffrey R. Comer[α‡], Mark D. Ginsberg[β] and Aleksei Aksimentiev[α,γ1]
[‡] These authors contributed equally to this work
[α]Department of Physics, University of Illinois, Urbana, IL
[β]US Army ERDC-CERL, Champaign, IL
[γ]Beckman Institute for Advanced Science and Technology,
University of Illinois, Urbana, IL

July 26, 2011

[1]corresponding author. Address: 1110 W. Green St., Department of Physics, University of Illinois, Urbana, IL 61801, U.S.A., Tel.: (1)-217-333-6495, Email: aksiment@illinois.edu

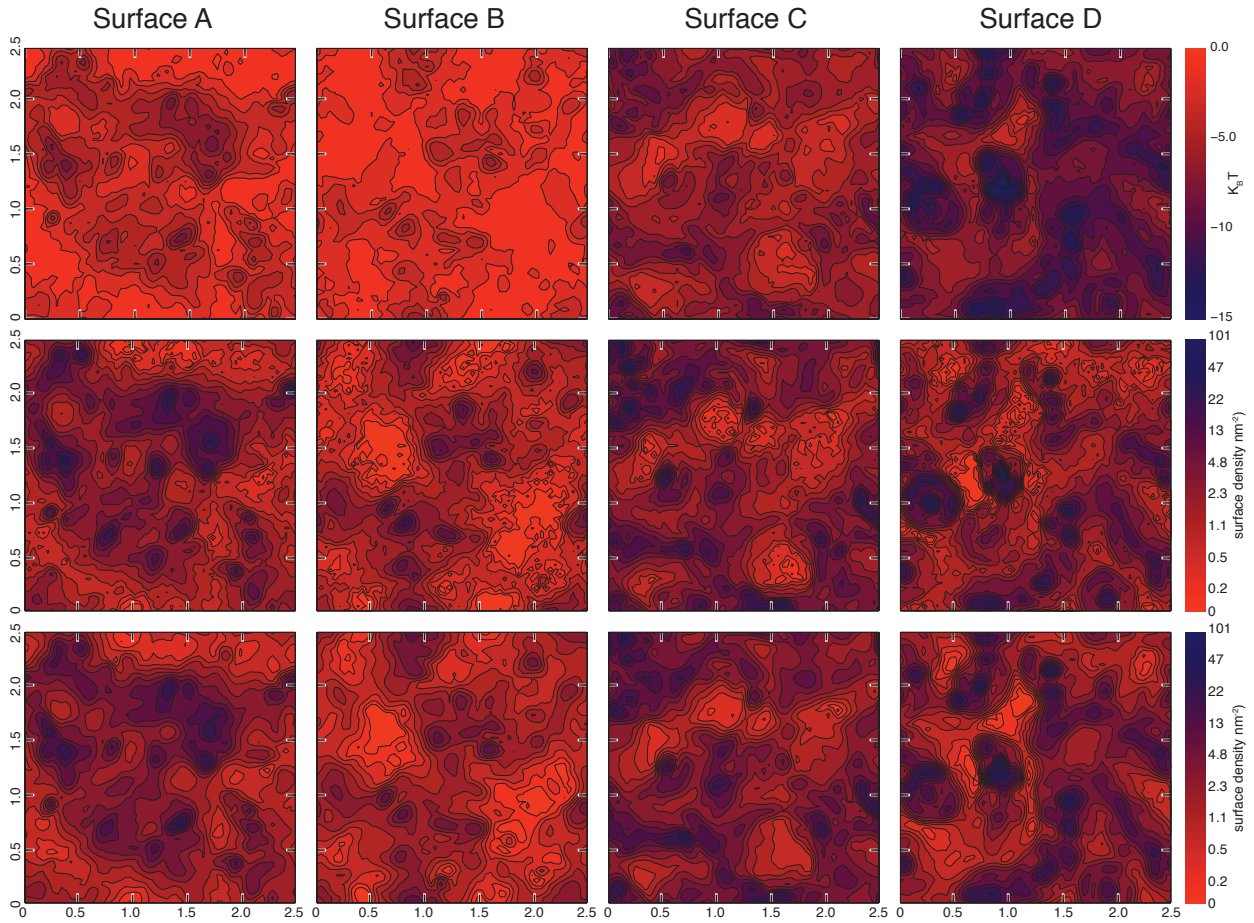

Figure S1: 2D maps of the DMMP–silica PMFs (top row) along with the surface density maps of adsorbed DMMP in MD (middle raw) and BD (bottom row) simulations. The resolution of each map is 0.42×0.42 Å^2. Note the logarithmic scale of the surface density maps. The results for the BD simulations represent the average of 25 unique trajectories starting from the same initial conditions as the one MD simulation.

All-atom models of silica surfaces and nanochannels. To produce atomic-scale models of silica membranes, we built a $2.5 \times 2.5 \times 3.5$ nm^3 block of crystalline silica containing 500 silicon and 1000 oxygen atoms by replicating a unit cell of SiO_2 [1]. The resulting system was annealed through NVT (constant number of particles N, volume V and temperature T) simulations for 20 ps at 7000 K, 20 ps at 5000 K, 50 ps at 2000 K, 100 ps at 1000 K, and 50 ps at 300 K. The annealing simulations, performed using the BKS potential [2,3] and a $2.5 \times 2.5 \times 5.5$ nm^3 periodic cell, produced an amorphous silica membrane with two relaxed surfaces. As in Vollmayer et al. [3], the form of the BKS potential was modified at small distances to prevent spurious behavior at high temperature. The Coulomb portion of the BKS potential was computed using the PME method [4], while the Lennard-Jones portion was smoothly shifted to zero at an interatom distance of 0.55 nm. During the annealing procedure, external forces were applied to prevent the atoms from evaporating into the vacuum region [5,6]. The temperature was controlled by Langevin dynamics with a damping constant of 5 ps^{-1}.

Using the results of the annealing simulations, we created four SiO_2 surfaces, each having different surface properties. Surfaces A and B were produced by removing atoms within 0.42 nm of either side of the membrane using the atomic coordinates obtained at the end of the annealing process. This produced thereby two different surfaces (surface A and B, Figure 3 a,b) having a structure similar to a cross section of amorphous silica. The resulting membrane, having surface A at the bottom and surface B at the top, was used to make nanochannel system AB through use of periodic boundary conditions. Nanochannel

system A was created by splitting the AB membrane horizontally in half, retaining only the bottom part of the membrane (containing only surface A). This part of the membrane became the top wall of nanochannel system A. The bottom wall of the nanochannel system A was created by replicating and rigidly transforming its top wall, producing a channel that had two identical surfaces (surface A) at the bottom and top.

The same replication and transformation procedure was used to produce nanochannel system C using the bottom half of the SiO_2 membrane with the atomic coordinates obtained at the end of the first annealing procedure (20-ps simulation at 7000 K). This system had similar properties to the system used in Carr et al.[7]. Nanochannel system D was made in the same way as nanochannel system C except that it was made using the atomic coordinates from the very end of the last annealing simulation (50-ps simulation at 300 K). Thus, surface D can be thought to have a more relaxed structure than surface C as it was annealed more thoroughly.

We used the BKS force field in the annealing simulations to produce different but plausible atomic structures of the SiO_2 surfaces. In the subsequent all-atom simulations of the nanochannel systems, the SiO_2 atoms were restrained to the positions generated by the annealing simulations[5,8,9]. The strength of the restraints and of the oxygen–silica bonds were chosen to give the membrane a dielectric constant of ~ 5. The restraint force was given by $\vec{F}(\vec{r}_i) = -2K(\vec{r}_i - \vec{R}_i)$, where $\vec{r}_i$ and $\vec{R}_i$ are the current and initial positions of atom i and $K = 13,900$ pN/nm. Bonds were established between all silicon and oxygen atoms separated by less than 0.22 nm; the bond spring constant $K_{\mathrm{bond}} = 695$ pN/nm. The interaction of the SiO_2 atoms with water and DMMP were calculated using the CHARMM compatible force field of Cruz-Chu et al.[8].

MD simulation setup All MD simulations of DMMP adsorption and transport were performed using atomic-scale models of silica nanochannels that contained DMMP solution enclosed between two surfaces (see Figure 1). As described above, nanochannel systems A, AB, C and D were created using silica membranes A, AB, C, and D, respectively, tiled in a four-by-four grid into larger membranes, each consisting of sixteen identical patches and measuring 10×10 nm^2 in total area. To make nanochannel AB, membrane AB was placed in a periodic box of the same width and breadth but of greater height than the membrane, which created a system that was effectively infinitely long and wide, with a gap of about 5.6 nm separating surface A and B (see Figure 1). Similar approach was used to build nanochannel systems A, C, and D that had identical top and bottom surfaces and thus 32 identical patches per system. The volume between the surfaces was then filled with a solution of DMMP. We used CHARMM-compatible parameters for DMMP previously described in Carr et al.[10].

Following a 2000-step minimization using a conjugate gradients method, each system was equilibrated for 1.5 ns in the NPAT ensemble (constant number of particles N, pressure P, area in the x-y plane A and temperature T). The membrane was oriented normal to the z axis of our coordinate system. During the NPAT simulation, some DMMP molecules may have adsorbed to the surfaces. To remove this effect, all DMMP molecules were moved back to their initial coordinates, and constrained to those coordinates for a 0.5 ns simulation in the NVT ensemble, removing any steric clashes between DMMP and water molecules. Each system was then simulated in the NVT ensemble with a pressure gradient induced in the x-direction, resulting in a pressure-driven flow of DMMP solution through the system. To induce a pressure gradient, a constant force in the x-direction F_x was applied to all N water molecules, creating a pressure difference ΔP_x across the system of

$$\Delta P_x = N \cdot F_x / A, \tag{1}$$

where A is the area of the chamber in the y–z plane[7]. Temperature was maintained by applying the Langevin thermostat to all silica atoms, which was sufficient to keep the temperature of the entire system within 1.2% of the target temperature[7]. To investigate whether the pressure-driven flow affected the amount of solute bound, we performed simulations of system A with and without the applied pressure difference, which showed that the pressure-driven flow had no measurable effect on adsorption[10].

Analysis of the BD and MD simulations To calculate the solute adsorption on the nanochannel surfaces, a DMMP molecule was considered adsorbed in an MD (BD) simulation if its phosphorus atom (center of mass), was within 0.5 nm of the surface. The surface of each silica membrane was defined as the x-y plane with the z coordinate determined as the average z coordinate of the isosurface defined by the five-to-one ratio of silica and water atoms in the MD simulation. To make the 2D surface density plots of

adsorbed solutes, such as shown in Fig. S1, each surface was partitioned into a grid with a 0.42×0.42 Å^2 grid size. The number of DMMP bound to each grid point was computed by analyzing the steady-state parts of the respective trajectories, averaging over all identical patches of the surfaces.

Umbrella sampling simulations. To characterize the interaction between a single DMMP solute and the membrane surfaces, we created four small systems consisting of a single silica membrane, water, and one DMMP molecule. The potential of mean force (PMF) of a DMMP molecule as a function of its position relative to the membrane surface was determined from a set of umbrella sampling simulations[11], which were analyzed using the weighted histogram analysis method (WHAM)[12] generalized to three dimensions (see below). Prior to the umbrella sampling simulations, each of the four systems underwent 2000 steps of energy minimization, 2 ps of equilibration at fixed volume during which the temperature was raised from 0 to 295 K by velocity rescaling, and 200 ps of NPT simulation.

The umbrella sampling simulations were performed by restraining the phosphorus atom of the DMMP molecule to points in (x, y, z) (where z is perpendicular to the surface) using the potential energy function $w_i(x, y, z) = \frac{1}{2}k_x(x - x_i)^2 + \frac{1}{2}k_y(y - y_i)^2 + \frac{1}{2}k_z(z - z_i)^2$, where (x_i, y_i, z_i) was the center of sampling window i and k_x, k_y and k_z were the spring constants along each axis. Because the gradient of the PMF was much larger along the z axis than in the xy plane, a stiffer spring constant of k_z =1390 pN/nm was used along the z axis than perpendicular to it, for which $k_x = k_y$ =70 pN/nm. Furthermore, the sampling windows (x_i, y_i, z_i) were more closely spaced along the z axis. The sampling windows formed a three-dimensional grid with 4, 4, and 9 points along the x, y, and z directions, respectively. Results were first obtained using the 144 sampling windows centered at these points, but to increase the resolution of our PMF distributions, we added another 300 sampling windows. For these simulations, we used a grid of 5, 5, and 12 points with spring constants $k_x = k_y = 560$ and $k_z = 2780$ pN/nm. To ensure that the calculated PMF extended into bulk water, 19 sampling windows with the same spring constant as the previous set were added to the (x,y) center of the membrane for an additional nanometer in z. Each simulation represented more than 2.2 ns. The first 0.2 ns of each simulation was excluded from the WHAM PMF calculation.

To calculate the PMF between two DMMP molecules, we created a simulation system containing two DMMP molecules and 3,426 water molecules, measuring $4.6 \times 4.6 \times 4.6$ nm^3. After a brief 1000-step energy minimization using a conjugate gradients method, the system was equilibrated for 0.2 ns in the NPT ensemble at 295 K. Umbrella sampling simulations were performed by restraining the distance between the phosphorus atoms with a potential energy function $w_i(\vec{r}_1, \vec{r}_2) = \frac{1}{2}k_r \left(|\vec{r}_1 - \vec{r}_2| - b_w\right)^2$. 40 sampling windows were used, varying the P–P distance b_w from 0.36 to 1.96 nm in 0.04-nm increments. The force constant of the harmonic restraints was $k_r = 5092$ pN/nm. Each sampling simulation lasted 6 ns. The first 0.2 ns of each simulation was excluded from the WHAM PMF analysis.

Potential of mean force calculation. The potential of mean force (PMF) was computed by the weighted histogram analysis method (WHAM) described by Roux[12], generalized to three dimensions. For our system, each of the three spatial dimensions is a reaction coordinate. We estimate the unbiased probability distribution by

$$\langle \rho(x, y, z) \rangle = \left(\sum_{i=1}^{N_w} n_i \, \langle \rho_i(x, y, z) \rangle \right) \left(\sum_{j=1}^{N_w} n_j \exp\left[-\frac{w_j(x, y, z) - F_j}{k_\mathrm{B}T} \right] \right)^{-1}, \tag{2}$$

where $\rho(x, y, z)$ is the unbiased probability distribution, N_w is the number of biased simulations, $\rho_i(x, y, z)$ is the biased probability distribution derived from the results of biased simulation i, n_i and $w_i(x, y, z)$ are the number of independent data points and the biasing potential, respectively, for biased simulation i, and $\{F_i\}$ is a set of constants.

The set of constants $\{F_i\}$ are initially unknown; thus, we make an initial guess for their values. After estimating $\langle \rho(x, y, z) \rangle$ by Equation 2, we can obtain improved estimates of these constants by solving

$$\exp\left[-\frac{F_i}{k_\mathrm{B}T} \right] = \int \mathrm{d}x \int \mathrm{d}y \int \mathrm{d}z \exp\left[-\frac{w_i(x, y, z)}{k_\mathrm{B}T} \right] \langle \rho(x, y, z) \rangle \, . \tag{3}$$

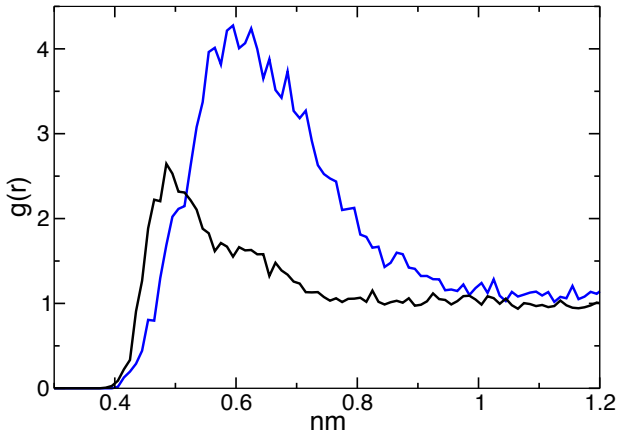

Figure S2: Radial pair distribution functions of DMMP simulated with all-atom (black line) and implicit-solvent (blue line) MD.

To obtain self-consistency, the equations are iterated, feeding the newest estimate of $\{F_i\}$ into Equation 2 and then the newest estimate of $\langle\rho(x,y,z)\rangle$ into Equation 3. Iteration ceases at iteration j when $\left|(F_{i+1}-F_i)^{(j)}-(F_{i+1}-F_i)^{(j-1)}\right| < 0.0001\,k_{\mathrm{B}}T$ for all windows $i \in \{1,2,...,N_w-1\}$. The PMF is then computed by $-k_{\mathrm{B}}T\log(\langle\rho(x,y,z)\rangle)$.

Implicit solvent MD simulations To compare our atomic-resolution BD method with implicit-solvent MD, we created a simulation system by removing all water molecules from the all-atom model of the nanochannel system *A*. Our implicit solvent simulations were performed using the Onufriev, Bashford, and Case (OBC) implicit solvent model[13]. The generalized Born radius for each atom[14] was taken to be half the distance at which the Lennard-Jones potential is zero[15] (one half the Lennard-Jones σ), and the HCT scaling factors were taken from Hawkins, Cramer and Truhlar (HCT)[16] and Tinker[17]. As no ready-to-use HCT scaling factors were available for silicon, several HCT factors were tested, including a low HCT scaling factor of 0.72 (same as HCT of carbon) and a high HCT scaling factor of 0.96 (same as HCT of sulfur).

All implicit-solvent simulations were performed using GROMACS 4 [18], a timestep of 2 fs with all bonds constrained by the P-LINCS algorithm[19], periodic boundaries, and an electrostatic and van der Waals cut-off of 2.5 nm. The implicit-solvent MD simulations only modeled the diffusion of solutes in the nanochannels, as no flow was induced. As discussed in Carr et al.[10], the presence of a flow does not affect the amount of solute adsorbed on the nanochannel surfaces for the range of flow velocities studied.

In our implicit-solvent MD simulations, the DMMP molecules were observed to aggregate in solution. Fig. S2 illustrates this behavior by comparing the radial pair distribution functions of DMMP in bulk solution simulated using all-atom and implicit-solvent MD methods. Thus, our implicit model of DMMP does not properly capture properties of a DMMP solution, which makes quantitative comparison of the results of DMMP adsorption simulations impossible. We note, however, that the overall amount of DMMP adsorbed at the silica surface strongly depends on the HCT scaling factor used to describe silicon, producing a finite concentration of adsorbed DMMP for an HCT scaling factor of 0.72 and no DMMP adsorption for 0.96.

While unable to quantitatively compare implicit solvent MD to all-atom MD in their ability to predict DMMP adsorption on silica with atomic-scale precision, we were able estimate the gain in performance from switching to the implicit solvent representation. In our simulations, the performance gain was rather moderate, as the entire silica surface was described in atomic details. Specifically, implicit solvent simulations produced ∼28 ns/day on 240 processors, which was only double the performance of all-atom MD with explicit water, ∼14 ns/day on 288 processors. Eliminating the all-atom description of silica would surely speed up implicit solvent simulations. It is, however, not clear if such a model could preserve atomic-scale information about the arrangement of surface atom, which is critical for proper description of the surface's local affinity to water. The latter was found to be the dominant factor governing DMMP adsorption in all-atom MD simulations[10].

Smoluchowski model. To compare the results of our BD simulations with a simple continuum model, we used the Smoluchowski equation to predict the density of solute bound to the nanochannel surfaces. The Smoluchowski equation,

$$\partial_t c\left(z,t\right) = \partial_z \left(\mathrm{D}\,\partial_z - \frac{F(z)}{\gamma} \right) c\left(z,t\right), \tag{4}$$

describes the time evolution of solution concentration c under an external force F, where D is the diffusivity of the particles, γ is the coefficient of friction in the solution, and $c\left(z,t\right)$ describes the probability of finding a particle at position z at time t. The Smoluchowski model describes the dynamics of the solute as diffusive motion in an external potential and ignores solute–solute interactions. Instead of solving the full 3D Smoluchowski equation, here we consider a quasi 1D system, where W_{PS} is simply a function of the distance from the surface. The effective one-dimensional PMF is be computed from the 3D PMF by integrating out the unused degrees of freedom:

$$W_{\mathrm{PS}}\left(z\right) = \frac{1}{L_x L_y} \int_0^{L_x} dx \int_0^{L_y} dy\; e^{-W_{\mathrm{PS}}(x,y,z)}. \tag{5}$$

To solve the Smoluchowski equation, we wrote custom routines in MATLAB[20]. For the external force, $F\left(z\right)$, we took the numerical derivative of the 1D surface–solute PMF, and interpolated the solution for the given z. We used reflective boundary conditions to conserve probability,

$$\mathrm{D}\left(\partial_z - \frac{F(z)}{k_B T} \right) c\left(z,t\right) = 0, \text{ at } z = 0, h \text{ nm} \tag{6}$$

where h is the length of the channel, and an initial probability distribution,

$$c(z=0, t=0) = 1/h, \text{ at } 1.25 \text{ nm} < z < (h - 1.25) \text{ nm} \tag{7}$$

corresponding to the initial conditions of our all-atom MD simulations. The density of adsorbed DMMP molecules predicted with the Smoluchowski model is shown in Figure 5. Due to the lack of inter-particle interactions, the Smoluchowski equation predicts a constant fraction of solutes adsorbing to the surface in each simulation. While this is valid for low concentrations, the model overestimates the amount of adsorbed solute at even moderate concentrations.

References

[1] A. Aksimentiev, R. Brunner, E. R. Cruz-Chu, J. Comer and K. Schulten, *IEEE Nanotechnology Magazine*, 2009, **3**, 20–28.

[2] B. W. H. van Beest, G. J. Kramer and R. A. van Santen, *Phys. Rev. Lett.*, 1990, **64**, 1955–1958.

[3] K. Vollmayr, W. Kob and K. Binder, *Phys. Rev. B*, 1996, **54**, 15808–15827.

[4] P. F. Batcho, D. A. Case and T. Schlick, *J. Chem. Phys.*, 2001, **115**, 4003–4018.

[5] J. Comer, D. B. Wells and A. Aksimentiev, *Protocols in DNA nanotechnology*, Humana Press, 2011, vol. 749, ch. 22, pp. 317–358.

[6] D. B. Wells, V. Abramkina and A. Aksimentiev, *J. Chem. Phys.*, 2007, **127**, 125101.

[7] R. Carr, J. Comer, M. D. Ginsberg and A. Aksimentiev, *IEEE Tran. Nanotechnol.*, 2011, **10**, 75–82.

[8] E. R. Cruz-Chu, A. Aksimentiev and K. Schulten, *J. Phys. Chem. B*, 2006, **110**, 21497–21508.

[9] J. Comer, V. Dimitrov, Q. Zhao, G. Timp and A. Aksimentiev, *Biophys. J.*, 2009, **96**, 593–608.

[10] R. Carr, J. Comer, M. D. Ginsberg and A. Aksimentiev, *J. Phys. Chem. Lett.*, 2011, **2**, 1804–1807.

[11] G. Torrie and J. Valleau, *Journal of Computational Physics*, 1977, **23**, 187–199.

[12] B. Roux, *Computer Physics Communications*, 1995, **91**, 275–282.

[13] A. Onufriev, D. Bashford and D. Case, *Proteins: Struct., Func., Bioinf.*, 2004, **55**, 383–394.

[14] N. A. Baker, D. Bashford and D. A. Case, *New Algorithms for 521romolecular Simulation*, Springer Berlin Heidelberg, 2006, vol. 49, pp. 263–295.

[15] P. Bjelkmar, P. Larsson, M. Cuendet, B. Hess and E. Lindahl, *J. Chem. Theory Comput.*, 2010, **6**, 459–466.

[16] G. Hawkins, C. Cramer and D. Truhlar, *J. Phys. Chem.*, 1996, **100**, 19824–19839.

[17] J. Ponder, *TINKER: Software Tools for Molecular Design*, 2009, `http://dasher.wustl.edu/tinker/`.

[18] B. Hess, C. Kutzner, D. Van Der Spoel and E. Lindahl, *J. Chem. Theory Comput.*, 2008, **4**, 435–447.

[19] B. Hess, *J. Chem. Theory Comput.*, 2008, **4**, 116–122.

[20] The MathWorks, Inc., *Matlab v.7*, 2008.